A Schrödinger-Poisson Solution of CNT-FET Arrays

A. Marchi, S. Reggiani and M. Rudan
Advanced Research Center on Electronic Systems (ARCES), and Dept. of Electronics (DEIS)
University of Bologna, Viale Risorgimento 2, I-40136 Bologna, Italy, tel. +39-051-209-3773
E-mail: amarchi@arces.unibo.it.

***Abstract*— In this work we investigate and compare the electrostatics of carbon-nanotube field-effect transistor (CNT-FET) arrays. To this purpose, we have developed a self-consistent Schrödinger-Poisson solver which fully takes into account quantum effects and the CNTs physical properties. We show that quantum effects have to be carefully taken into account in order to properly catch the electrostatic behavior of these devices. A further analysis is carried out in order to quantify the screening effects that arise when an array of nanotubes in parallel is used, showing that such effects play a fundamental role in the electrostatic performance of CNT-FET arrays.**

I. Introduction

Carbon nanotubes (CNTs) are emerging as candidates for future nanoscale electronics. A number of CNT-FETs have recently been reported and investigated: among them, the gate-all-around (GAA), the top gate (TG) and the bottom-gate (BG) structures have been identified as the most promising architectures [1]. The understanding of the behavioral and performance issues of such devices requires an accurate analysis of the electrostatics: in fact, the charge induced by the gate is related to the transistor's on-current and to the gate-to-channel capacitance that directly contributes to the device transconductance. In order to make CNT-FETs competitive with respect to conventional FETs, arrays of nanotubes should be used [2]. The geometrical distribution and relative distances between CNTs in the array lead to screening effects that need to be accounted for: as a consequence, it is not sufficient to investigate the single-nanotube electrostatics. Wang et al. [3] presented a simulative analysis of the electrostatics of a CNT array by modeling the nanotubes as ideal metal rings. This approach provides a qualitative trend for the gate-to-channel capacitance as a function of the packing density, but does not allow for the inclusion of the specific physical properties of the nanotubes. In order to quantitatively investigate the electrostatics of CNT-FET devices, we have developed a self-consistent 2D Schrödinger-Poisson solver which fully accounts for the nanotube electronic properties (e.g., 1D density of states) and for the quantum distribution of charge along the circumference of the CNT; the numerical details are given in the following section. As an example of application, we show the influence of the 1D density of states and of the quantum effects on the gate capacitance, along with the screening effects that arise when the CNTs are packed together. The results are discussed in Section III and compared with those obtained in [3], while in Section IV the conclusions are drawn.

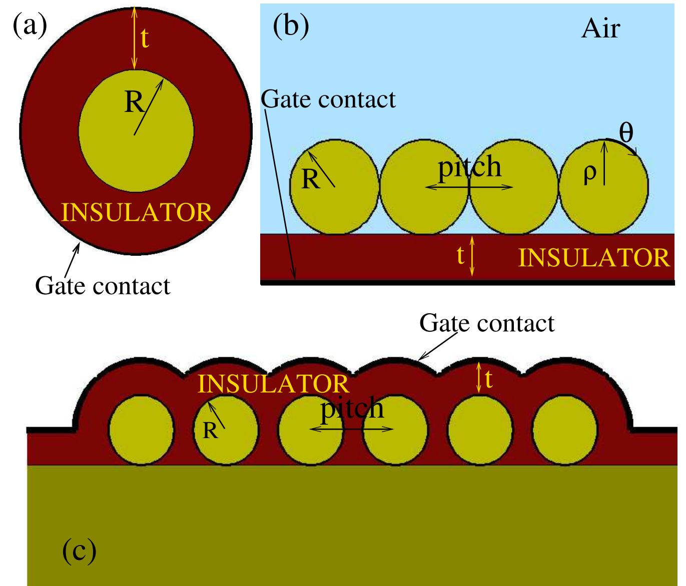

Fig. 1. The architectures under investigation: (a) Gate-all-around; (b) Bottom gate; (c) Top gate. The geometrical parameters and the local reference system ρ, θ used for the Schrödinger solution are shown. The pitch is defined as the distance between the centers of two adjacent CNTs.

II. Numerics

The numerical solver described below is used to analyze the electrostatic behavior on a cross section along the channel of the CNT-FET devices, assuming zero source and drain voltages. In the case of a single GAA CNT-FET, the problem can be tackled by means of a one-dimensional approach, since there is no dependence of the charge on the angular coordinate [4], [5]. If the cylindrical simmetry is lost, e.g., by choosing a different architecture or by introducing an array of nanotubes, a fully 2D approach is necessary for the Poisson equation, whereas a 1D cylindrical Schrödinger equation is applicable on each circumference representing a CNT, since the charge is localized at the surface of the nanotube. For a given geometry, the set of 1D Schrödinger equations is solved self-consistently with the 2D Poisson equation over the whole domain. This yields:

$$-\nabla \bullet [\varepsilon(x,y)\nabla\phi(x,y)] = \sum_i (-qn_i)\,, \qquad (1)$$

$$-\frac{\hbar^2}{2\mu_i}\frac{\mathrm{d}^2\psi_{mi}(s)}{\mathrm{d}s^2}+V_i(s)\psi_{mi}(s)=E_{mi}\psi_{mi}(s),\ s=R_i\theta \quad (2)$$

where ε is the point-dependent dielectric constant, ϕ the electrostatic potential, and n_i the electron concentration of the ith CNT. We assume intrinsic nanotubes. The Schrödinger equation on the ith CNT is solved by introducing a local cylindrical reference system (ρ, θ) (see Fig. 1): R_i is the CNT radius, ψ_{mi} and E_{mi} the mth eigenfunction and eigenvalue, respectively, and $V_i = -q\phi_i$ the electrostatic potential energy of the ith nanotube. The angular effective mass μ_i is fitted for each nanotube in such a way that, when no external potential is applied, E_{0i} and E_{1i} given by the solution of (2) correspond to the energy band gap and to the first subband energy level for the specific CNT, respectively, as indicated by the universal density of states of [6]:

$$E_{0i}=E_g/2=\frac{|V_{pp}|a_{cc}}{2R_i}\,, \qquad E_{1i}=\frac{|V_{pp}|a_{cc}}{R_i}\,. \quad (3)$$

In the latter, V_{pp} is the nearest-neighbour interaction potential, a_{cc} the carbon-carbon bond distance and E_g the nanotube energy band gap. The fitting is accomplished by taking $\mu_i = \hbar^2/(|V_{pp}|a_{cc}R_i)$. It has been verified that, at the dimensional sizes analyzed in this work, only the first two energy subbands contribute to the charge density: therefore, this choice for μ_i guarantees that the electronic properties of the CNTs are fully accounted for. As positive gate voltages are considered, only electrons contribute significantly to the total charge density. The local electron concentration of the ith nanotube is computed as:

$$n_i(\rho,s)=\sum_{m=0}^{\infty}|\psi_{mi}(s)|^2\delta(\rho-R_i)\times$$
$$\int_{E_{mi}}^{\infty} g(E;E_{mi})f(E;E_F)\mathrm{d}E \qquad [\mathrm{cm}^{-3}]\,, \quad (4)$$

where $f(E;E_F)$ is the Fermi function and $g(E;E_{mi})$ the 1D density of states along the axial direction z:

$$g(E,E_{mi})=\frac{8}{3\pi|V_{pp}|a_{cc}}\frac{E}{\sqrt{E^2-E_{mi}^2}}\,, \qquad E>E_{mi}\,,$$

This expression derives from a first-order expansion of the graphene two-dimensional band structure near the corners of the Brillouin zone [6]. The Fermi level E_F is pinned to the mid-gap of each nanotube.

III. Results

A cross-section of the analyzed architectures is shown in Fig. 1: (a) GAA CNT-FET, (b) BG CNT-FET, (c) TG CNT-FET. The radius R of the CNTs has been fixed to 0.7 nm. An equivalent oxide thickness t of 0.7 nm, and a power supply voltage of 1 V have been used, which are compatible with the 45 nm ITRS node specs [7] for ultra-thin SOI devices. Figure 2 (left) compares the electron density per unit length N_e as a function of the gate voltage V_G for the three structures with a single nanotube. In the subthreshold region, the electron density exponentially increases with the ideal slope of 60 mV/decade for the three devices. As expected, above threshold the GAA structure shows the largest charge-handling capability, due to its simmetry that allows for a better effectiveness of the gate control. The BG structure shows the lowest N_e (30% of the GAA case) while the TG one shows an N_e about 80% of the GAA case.

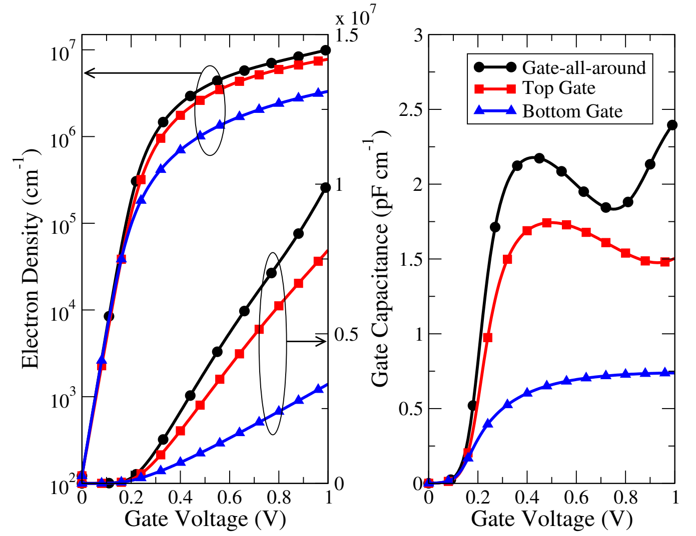

Fig. 2. Electron density (left) and gate capacitance (right) per unit length as functions of the gate voltage for the three structures with a single nanotube.

The gate capacitance per unit length $C_g = -q\,dN_e/d\,V_G$ as a function of the applied gate voltage is shown in Fig. 2 (right): the bump found for the GAA and TG architectures is related to the semiconductor capacitance of the device, which in turn is dominated by the filling-up of subbands (quantum capacitance). This effect can be ascribed to the one-dimensional nature of the nanotube and to the spacing of the subband energy levels. As V_G increases, the number of additional electronic states per unit energy decreases, leading to the decrease of C_g. When new energy levels are intersected by the Fermi level, the gate capacitance increases again. The latter is given by the series of the insulator capacitance and the semiconductor one: when the electrostatic coupling is better, the insulator capacitance is higher and its contribution to the series is lower. Consequently, the semiconductor capacitance, that is the only term that exhibits a bump, dominates the series when a better electrostatic coupling is reached, as in the case of a GAA or a TG configuration. This effect has to be carefully taken into account for an accurate determination of the device transconductance.

In order to make CNT-FETs competitive with state-of-the-art silicon devices, an appropriate number of nanotubes should work in parallel so as to correspond to the lateral dimensions of existing silicon devices. When an array of nanotubes is used, screening effects play an important role, and need to be taken into account to correctly predict the performance of the device. Figure 3 compares the electron density and

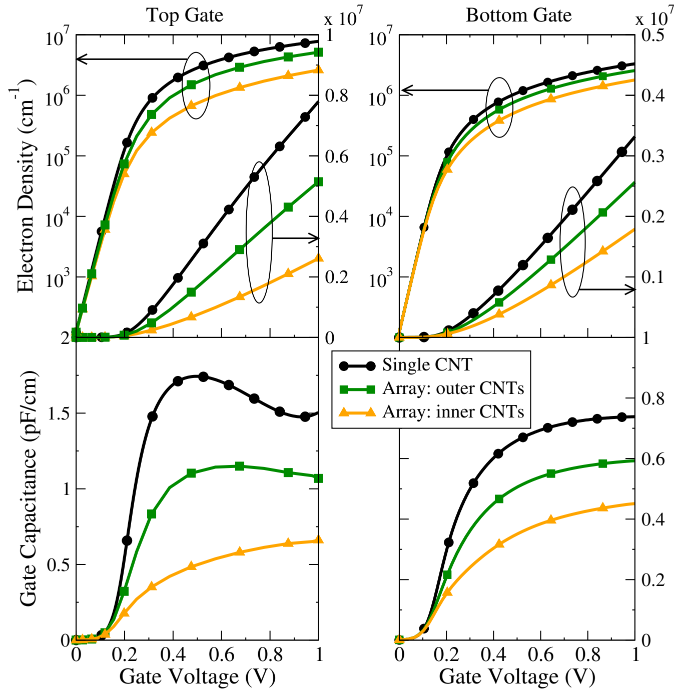

Fig. 3. Electron density (top) and gate capacitance (bottom) per unit length as functions of the gate voltage for the single nanotube device compared to those of the inner and outer tubes of an array of closely packed CNTs. Left: TG geometry; right: BG geometry.

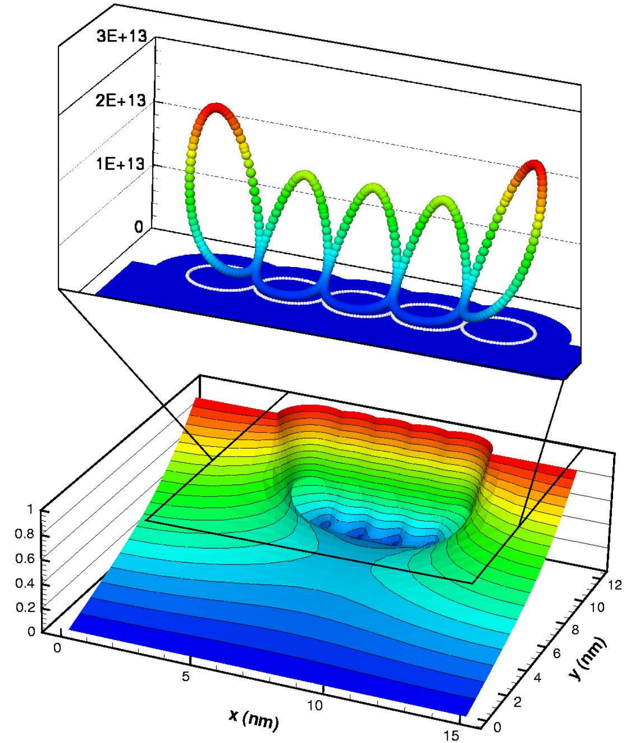

Fig. 4. 3D plot of the electron density per unit area (top) and of the electrostatic potential (bottom) at $V_G = 1$ V for an array of five nanotubes in the top gate configuration.

the gate capacitance per unit length of a single nanotube device to those obtained for the outer and inner tubes of an array of closely packed CNTs (pitch $= 2R$), both for the TG and BG architectures. The inner tubes experience a stronger screening effect than the outer ones: in the TG configuration, the electron density for the outer and inner tubes is 65% and 35% of that of a single-nanotube device, respectively. In the BG configuration, the reduction is less pronounced due to the weaker electrostatic coupling (80% and 55%, respectively) that is related to the lower effective dielectric constant of the material (air+insulator) surrounding the nanotubes.
Since our calculations include the electronic properties of the nanotubes, the gate capacitance we find (Fig. 3, bottom) is about 35% smaller than that obtained by treating CNTs as ideal metals [3]. Furthermore, it is interesting to note that the screening effects eliminate the bumps in the gate capacitance. The screening effects are also visible in Figs. 4 and 5, where a 3D plot of the electron density per unit area and of the electrostatic potential at $V_G = 1$ V are reported for the TG and BG geometries, respectively. One notes that, due to the stronger screening, the electron density of the inner tubes is lower than that of the outer ones. Furthermore, as mentioned above this difference is higher in the TG configuration due to the better electrostatic coupling between the tubes of the array. In fact, the peak of the electron density of the inner tubes is about 50% that of the outer ones in the TG configuration, while it is about 25% in the BG geometry. By increasing the number N of CNTs in the array, one finds that N_e depends linearly on N, and increases with a rate of about $0.24 \times 10^7\,\text{cm}^{-1}$ and $0.17 \times 10^7\,\text{cm}^{-1}$ per nanotube at $V_g = 1$ V for the TG and BG case, respectively. The linear dependence is confirmed by the fact that the electron densities per unit area of the inner tubes shown in Figs. 4 and 5 are almost the same.
As far as the electrostatic-coupling dependence on the pitch value is concerned, the analysis of the TG configuration has been carried out by changing the inter-CNT distance. We found that the maximum gate capacitance per unit area is given by a pitch of about $2(t + R) = 2.8$ nm (Fig. 6, top).
In fact, as the pitch increases, screening effects are reduced, the gate capacitance per tube increases consequently, but the occupied area increases as well. This means that an optimum pitch can be found in order to get the best trade off between the occupation area and the gate capacitance. It is worth noting that quantum effects play a dominant role in the determination of the optimum pitch: in fact, the gate capacitance bumps are more pronounced when better electrostatic coupling is achieved, that is, as the pitch increases and the screening lowers correspondingly. The larger oscillations at the optimum pitch make the gate capacitance per unit area lower than that of a closely-packed array at, e.g., $V_g = 1$ V. This is clearly shown in the inset of Fig. 6, which shows the gate capacitance per unit area as a function of the normalized pitch both at its maximum value and at $V_g = 1$ V. Finally, special care has been devoted to the analysis of the threshold voltage V_T

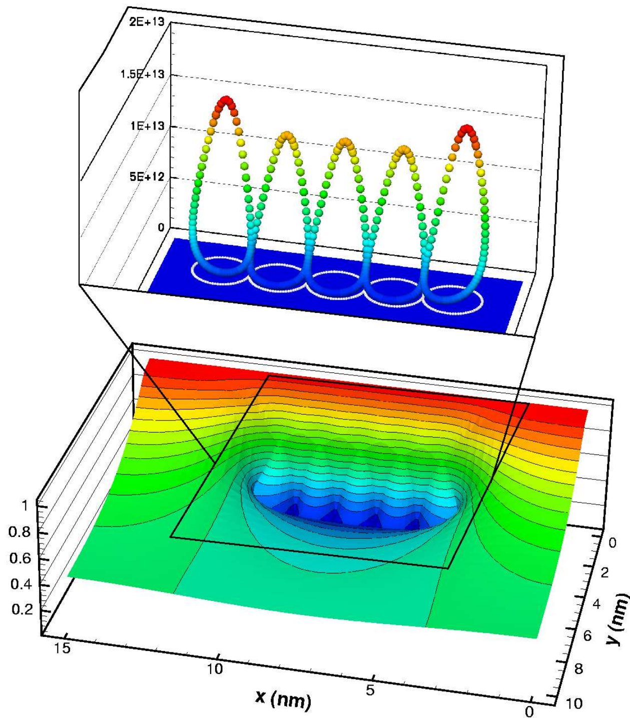

Fig. 5. 3D plot of the electron density per unit area (top) and of the electrostatic potential (bottom) at $V_G = 1$ V for an array of five nanotubes in the bottom gate configuration.

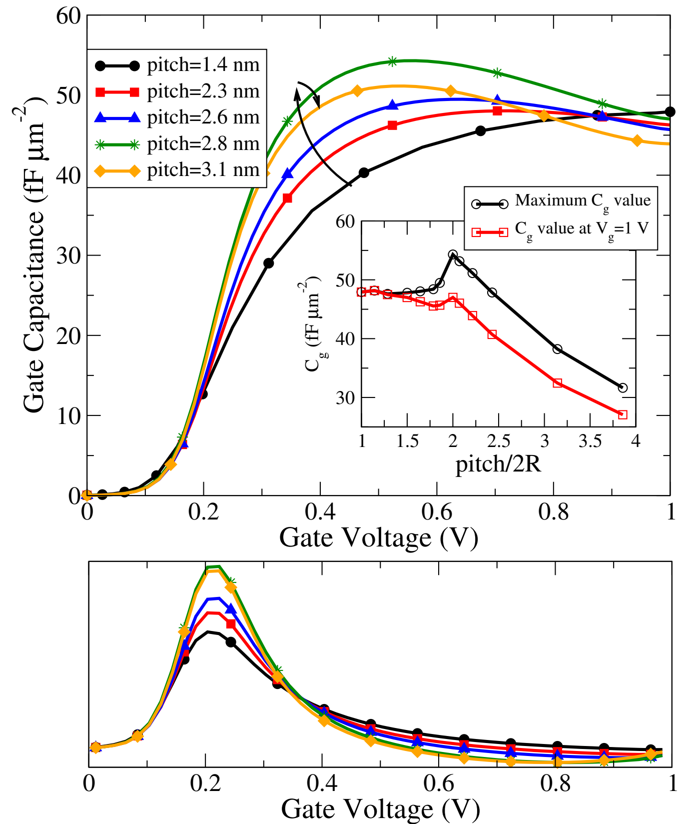

Fig. 6. Top: gate capacitance per unit area as a function of the gate voltage for different pitch values for the TG geometry. The arrows indicate the direction of increasing pitch. The optimum pitch is around 2.8 nm. Inset: maximum value and value at $V_g = 1$ V of the gate capacitance per unit area as a function of the normalized pitch value. Bottom: derivative of the gate capacitance per unit area.

of the CNT-FET array: as V_T is dominated by the electronic properties of the nanotube, we found that it is independent of the pitch value and of the number of CNTs constituting the array, as visible at the bottom of Fig. 6, where the maximum derivative of the gate capacitance is the same, irrespective of the pitch value.

IV. Conclusions

In this paper we have investigateted the electrostatics of GAA, TG and BG CNT-FETs and CNT-FET arrays at dimensional sizes compatible with the 45 nm ITRS node. This study shows that quantum effects have to be carefully taken into account in order to properly catch the electrostatic behavior of these devices. More specifically, the gate capacitance of the GAA and TG architectures shows a bump, that is not present in the BG configuration. Since the bump is more evident when a good electrostatic coupling is reached, it does not show up in the array of CNTs, because screening effects lower the gate-to-nanotube coupling. Moreover, the lowering of the electron density per nanotube in the array is more pronounced in the TG configuration with respect to the BG one. An optimum pitch exists in the top gate configuration that maximizes the gate capacitance per unit area, but a careful design is necessary since quantum effects make it to depend on the gate voltage. Finally, we found that the threshold voltage of an array is independent of the number of nanotubes and the distance between them, as V_T is strongly dependent on the electronic properties of the CNTs. The outcome of our approach provides an insight of CNT-FET features relevant for future nanoscale electronics.

Acknowledgments

This work has been partially supported by the EU IST Network SINANO (contract n. 506844).

References

[1] R. Martel *et al.*, in *IEDM Tech. Digest*, December 2001, pp. 159–162.

[2] R. Seidel *et al.*, *Nano Letters*, vol. 4, no. 5, pp. 831–834, 2004.

[3] X. Wang *et al.*, in *Proc. of SISPAD*, 2003, pp. 163–166.

[4] J. Guo *et al.*, *Appl. Phys. Lett.*, vol. 81, no. 8, pp. 1486–1488, August 2002.

[5] A. Marchi *et al.*, in *Proceedings of ULIS 2005*, Bologna, Italy, April 7-8 2005, pp. 99–102.

[6] J. W. Mintmire and C. T. White, *Phys. Rev. Lett.*, vol. 81, no. 12, pp. 2506–2509, September 1998.

[7] http://public.itrs.net, 2003.